Dynamics of High-Power Multi-Rotor System

Rafal P. Jastrzebski, *Member, IEEE,* Atte Putkonen, Eerik Sikanen, Andrei Zhuravlev, Tuhin Choudhury, Emil Kurvinen, Juha Pyrhönen, *Senior Member, IEEE*

***Abstract*—Typically, active magnetic bearings have been applied to high-speed rotors in medium to high power range to replace ball, roller, and oil-film bearings. They require less maintenance and provide number of unique benefits owing to contactless suspension and active control. Integrated compressor or turbines result in predictable rotor dynamics. This allows use of model-based controllers. The model-based centralized controllers outperform decoupled transfer function controllers, but they do require accurate plant models. For integrated wheels on a single rotor the control models comprise a rigid rotor and lowest frequency bending modes. The bending mode parameters related to node locations can be identified yielding controllers tuned to the applications. This work introduces drive train modelling and magnetic levitation control of 2 MW rotor and external load with flexible coupling. The model-based control is tested in the experimental setup and drive train frequency responses are compared to the modelled multi-rotor drive train dynamics.**

***Index Terms*—Magnetic bearings, Magnetic levitation, High-speed, Induction motor, Finite element analysis, Heat pumps, System dynamics, Variable speed drives, Flexible structure.**

I. Introduction

HIGH-SPEED and high-power electric machines are promising technology, which seeks to provide efficient and compact solutions for industry applications, such as compressor, blower, chillers and heat pump applications [1]. Especially active magnetic bearing (AMB) technology is promising in these applications, giving the possibility to influence to the operation actively and observe the behavior with high sampling frequency. The controlling of the AMB is typically model based, i.e. dynamical model is existing already in the system design phase. This is especially attractive and enables possibilities with the recently actively researched (detailed control system models branded) digital twins, where the virtual counterpart of the product is extensively utilized throughout the lifetime of the product and supports the operation [2]. Currently the models used to develop the controllers in AMB applications are not utilized after the R&D phase.

Authors would like to thank European Regional Council of South Karelia (decision numbers: A73086, A73066) and Business Finland (decision number: 6678/31/2019) for funding the projects. Authors would like to express their gratitude to technical and engineering teams behind the laboratory PoC construction.

R. P. Jastrzebski, A. Putkonen, A. Zhuravlev, and J. Pyrhönen are with Department of Electrical Engineering, Lappeenranta-Lahti University of Technology LUT, Yliopistonkatu 34, 53850 Lappeenranta, Finland. Rafal.Jastrzebski@lut.fi

E. Kurvinen is with Materials and Mechanical Engineering University of Oulu, Pentti Kaiteran katu 1, 90570 Oulu, Finland.

T. Choudhury and E. Sikanen is with Department of Mechanical Engineering, Lappeenranta-Lahti University of Technology LUT, Yliopistonkatu 34, 53850 Lappeenranta, Finland.

For example, this is important from the condition monitoring and maintenance perspective, as it forms the basis for system identification [3]; and enables comparison of the system behavior in respect to the model. For fault identification purposes the virtual counter part can be utilized to explore the parameters sensitivity and then generate data for example for neural networks [4].

In addition to its main function as a maintenance free bearings, the AMBs can be used to control vibrations, e.g. analysing and developing a vibration modelling [5], suppression and investigation of vibrations [6], [7], and compensating runout [8].

In the integrated applications the AMB's have been utilized for decades, e.g. in compressor applications [9]. However, the scalability of the solutions for higher power and speed faces limitations in many applications, as the mechanical rigidity, thermal load and dynamical behavior are compromised. Therefore, the upscaling design for higher power and speed requires completely new design. The process is multidisciplinary, convoluted, laborious and demands highly skilled team to be accomplish, e.g. in [10], [11] and [12].

To enable better modularity of the design and broader applicability of the single machine variant, in this study, the generalization of AMB supported motor is investigated. We use a case study of a multi-megawatt (MMW) AMB-rotor that has been introduced in [13], [14] and [11]. The modularity is achieved by using flexible coupling which can be tailored for the application specific needs, and enables utilization of the same driving motor for various applications. The flexible connection does change the system dynamics, which is then influencing the AMB control performance; but the needed changes to the controller are easily manageable while the driving machine variant remains unchanged. This provides significant advantage over needed machine redesign when using rotor integrated turbine or compressor wheels, however modelling of multi-rotor system is challenging.

This kind of analyses have not been presented before. In particular, multi-rotor drive trains with AMBs have not been analyzed from levitation control perspective. The related studies included [15] where multiple active magnetic bearings was utilized, however, the identification algorithm was demonstrated with two radial AMBs supporting single rotor. In [16] a trial misalignment approach for misalignment identification was proposed. In [17] two coupled Jeffcott rotors, supported with rolling element bearings and an auxiliary AMBs for fault identification were analyzed. [18] proposed methodology for identification of a flexible rotor. The control-

lability of a flexible rotor for various unbalance was advanced in [19], e.g. for unbalance and harmonic disturbance of flexible rotor. Also an frequency domain control-relevant identification of MIMO AMB rigid rotor was shown in [20].

In this work, modelling of multi-rotor system is in focus and methods to advance the design are explored. The control design and operation of coupled AMB system is investigated and tested. We propose control methodology for the case where flexible coupling is used to connect the motor to the application; and the dynamics change is handled with the control of AMBs. Analyses and experiments show that the dominant bending mode frequencies will be reduced while modal damping factors will increase.

II. Modelling of coupled drivetrain

The initial controller employs the linearized control plant model of the AMB-rotor alone with added left-end flange of the coupling as a point mass (see Fig. 2). In the controller the most outer radial AMBs and an axial AMB are actively used. This results in classical centralized 4 degrees-of-freedom (DOF) radial controller and 1 DOF axial controller. For time domain verifying simulations a nonlinear plant model is derived. It comprises speed dependent mechanical model of the whole drive train and the nonlinear actuators implemented as look-up-tables (LUTs) based on electromagnetic finite element method (FEM) models. The FEM derived mechanical models use modal reduction to retain the number of lower frequency bending modes represented in the plant to limit computational burden.

A. Mechanical rotor models

The equation of motion is derived based on FEM. The rotor shaft is discretized into three-dimensional beam elements along its axis of rotation based on Timoshenko's beam theory [21], as shown in Fig. 1. Each rotor node has two translational and two rotational degrees of freedom (DOF). Discs, such as axial AMB rotor and lock nuts, are simplified and added as mass points in their corresponding node location.

From the FEM interface point of view, the geometry, material, and physical parameters of the rotor contribute as input to the each rotor model in a drive train (MMW, RENK, Rotatek). The FE models of each component of the drive train are tuned individually to match their experimentally measured natural frequencies.

For the active part of the MMW, the 3-D beam elements are unable to represent the complicated slit rotor structure. Therefore, the cross-sectional properties of the active part are calculated from the CAD model and updated in the FEM model. The radial spacers, lock nuts, and axial AMB disc are introduced as mass points. The AMB, sensor lamination, and slit rotor section properties (such as elasticity and density) can be updated based on measured frequency responses for increased accuracy.

In the RENK coupling flanges and hollow tubular section are defined as beam elements. The flanges on either side are

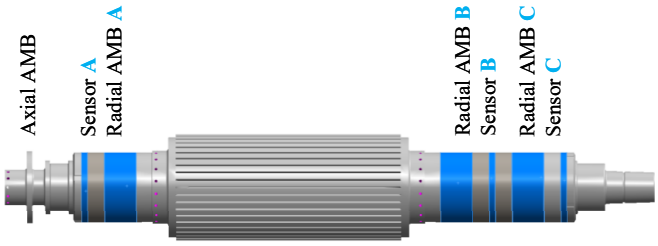

Fig. 1. Rotor layout with sensor and AMB lamination in blue. Three rotor balancing planes are marked with light purple dots.

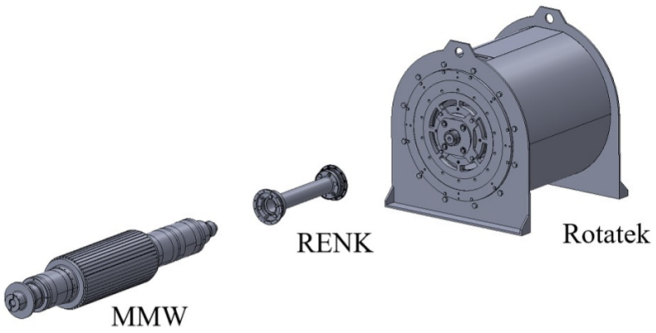

Fig. 2. Overview of the drivetrain comprising MMW solid slit rotor with AMBs connected by RENK coupling to the external load (Rotatek).

connected to the central hollow tube section via thin plates. These plates, which contribute to the overall flexibility of the coupling, are modeled as springs with properties tuned to the directional stiffness provided in the manufacturers catalogue.

Similar simplifications are also performed for the external load Rotatek machine.

Fig. 4a shows the first four mode shapes and their corresponding frequencies for the MMW and the coupling, respectively.

From the fundamental modelling point of view, the dynamics of elastic rotors can be generalized as a sum of the elastic and inertial forces acting on a beam. For Euler beam equation (no share deformation and equatorial mass moment of inertia density small), free bending vibrations in yz plane follow partial differential equation along z in time t

$$EJ\frac{\partial^4 w}{\partial z^4} = q, \tag{1}$$

where q, w, and EJ are the force per unit length, deflection of the beam in the y direction, and the stiffness respectively.

For Timoshenko homogeneous beam of constant cross-section the force per unit length affecting the displacement of the beam w is decreased due to share.

$$EJ\frac{\partial^4 w}{\partial z^4} = q(z) - \frac{EJ}{\kappa A G_1}\frac{d^2 q}{dz^2}, \tag{2}$$

with G_1 being shear modulus. κ and A are Timoshenko shear coefficient and cross section area.

Using separation of solution in time and space, supplementing boundary conditions of a bar element attachments,

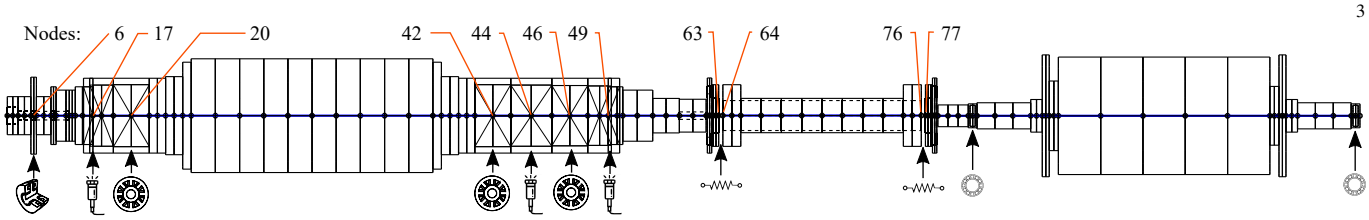

Fig. 3. FEM model of the drive train showing the node locations of Axial AMB, sensors, radial AMBs, ball bearings in load machine, and coupling springs. The Rotatek load machine uses ball bearings with combined enforced oil lubrication and cooling enabling high speeds.

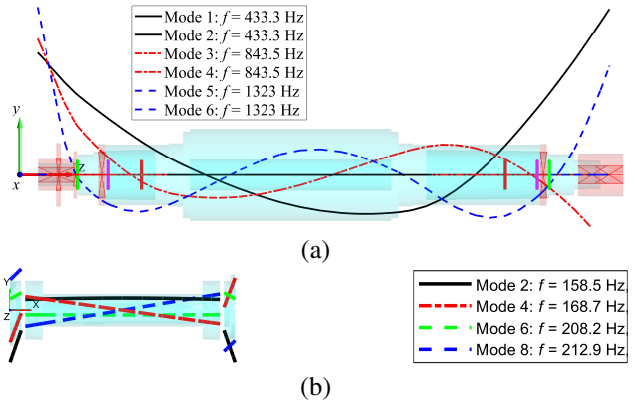

Fig. 4. The retained mode shapes and their respective frequencies for (a) MMW rotor (b) Coupling.

and initial conditions for the displacement and velocities the solution can be determined. The solution consists of infinite sum of eigenfunctions described by natural frequencies ω_i, $i = 1...\infty$ and eigenvectors defining unique mode shapes with arbitrary amplitudes.

After modal reduction the modal rotor dynamics comprise the rigid body modes and the dominant bending rotor modes. The number of dominant bending modes with the lowest natural frequencies is retained. The time behavior of each natural vibration follows a second order resonator. For example, we describe the first bending mode (i.e. the banana mode of the MMW in Fig. 4a) – the one with the lowest natural frequency as

$$m_1\ddot{y}_1 + d_1\dot{y}_1 + k_1 y_1 = 0 \tag{3}$$

$$d_1 = 2\zeta_1\omega_1 m_1, k_1 = \omega_1^2 m_1. \tag{4}$$

ζ_1 is the relative damping. m_1, d_1, and k_1 are modal mass, absolute damping, and stiffness.

Imposing state variables equal to vector of displacements [rigid rotor modal displacements in center of gravity (COG) coordinates and modal displacements] and velocities, the control plant in the state variable form with the control current vector as input and the rotor displacement vector at sensor locations as output is

$$\eta = \begin{bmatrix}\mathbf{x} & \dot{\mathbf{x}}\end{bmatrix} \tag{5}$$

$$\dot{\eta}=\mathbf{A}_\mathrm{r}\eta+\mathbf{B}_\mathrm{r}\mathbf{u}, \mathbf{y}=\mathbf{C}_\mathrm{r}\eta \tag{6}$$

$$\mathbf{A}_\mathrm{r} = \begin{bmatrix} \mathbf{0} & \mathbf{1} \\ -{\mathbf{M}_\mathrm{m}}^{-1}\left(\mathbf{K}_\mathrm{m} - \mathbf{T}_\mathrm{a}^\mathrm{T}\mathbf{K}_x\mathbf{T}_\mathrm{b}\right) & -{\mathbf{M}_\mathrm{m}}^{-1}\left(\mathbf{D}_\mathrm{m} + \Omega\mathbf{G}_\mathrm{m}\right) \end{bmatrix}$$

$$\mathbf{B}_\mathrm{r} = \begin{bmatrix}\mathbf{0} & {\mathbf{M}_\mathrm{m}}^{-1}\mathbf{T}_\mathrm{a}^\mathrm{T}\mathbf{K}_i\end{bmatrix}^\mathrm{T}, \mathbf{C}_\mathrm{r} = \begin{bmatrix}\mathbf{T}_\mathrm{s} & \mathbf{0}\end{bmatrix}.$$

When adding the first bending mode, the displacements at sensor and at actuator nodes depend on the mode shape and its nodal locations. These can be determined from FEM or experimentally together with modal damping and stiffness. The modal mass scales the modal amplitudes. For axi-symmetric rotor xz- and yz-plane dynamics are identical. The rotor mass, stiffness, damping matrices, and state variable vector in the COG modal coordinates are

$$\mathbf{M}_\mathrm{m} = \mathrm{diag}\left(m, m, I_x, I_y, m_1, m_1\right)$$

$$\mathbf{D}_\mathrm{m} = \mathrm{diag}\left(0, 0, 0, 0, d_1, d_1\right)$$

$$\mathbf{K}_\mathrm{m} = \mathrm{diag}\left(0, 0, 0, 0, k_1, k_1\right)$$

$$\mathbf{x} = \begin{bmatrix}x & y & \varphi_x & \varphi_y & x_1 & y_1\end{bmatrix}^\mathrm{T}.$$

The AMB stiffness matrices $\mathbf{K}_i$ and $\mathbf{K}_x$ are of diagonal form. Ω is rotational frequency.

The forces and moments enter the plant through the AMB locations while rotor displacements are measured at sensor locations. The $\mathbf{T}_\mathrm{a}$ and $\mathbf{T}_\mathrm{s}$ are transformation matrices of the coordinates from the COG of the rotor to the sensor and actuator frames respectively.

$$\mathbf{x}_\mathrm{a} = \mathbf{T}_\mathrm{a}\mathbf{x}, \mathbf{x}_\mathrm{s} = \mathbf{T}_\mathrm{s}\mathbf{x} \tag{7}$$

The forces and moments in bearing frame follow the transformation to the COG of the rotor frame

$$\mathbf{F} = \mathbf{T}_\mathrm{a}^T\mathbf{F}_\mathrm{a}. \tag{8}$$

The model (6) is linear except for the case with the variable speed Ω.

B. AMB models

The linearized control plant model embeds the bearing current stiffness and position stiffness together with the reduced modal mechanical rotor dynamics in the state space form (6). For example the linearised forces along the control x axis are

$$F_x = k_i i_{cx} + k_x x. \tag{9}$$

The current stiffness k_i and position stiffness k_x are defined at the operating point ($x = 0$, $i_c = 0$) where the analytical expressions are generalized assuming no saturation, no fringing flux paths and force geometric decoupling.

$$k_i = \frac{\mu_0 N^2 S \cos\xi i_b}{l_0^2}, k_x = \frac{\mu_0 N^2 S \cos\xi i_b^2}{l_0^3}, \quad (10)$$

where ξ is the geometric force acting angle, N is the number of turns, l_0 is mean airgap, and μ_0 is permeability of air. However, the more accurate values are taken from electromagnetic FEM simulations (see Fig. 5) or measured experimentally [14]. Additionally, inner current controlled closed-loop dynamics can be identified from the experimental frequency responses. Consequently, the inner loop dynamics can be added in series to the rotor dynamics in the complete control model.

The linerized plant models are used for the control synthesis. For control validation the nonlinear plant is applied. It comprises rotor dynamics with force and speed inputs, and AMB force maps. To ease the computational burden in the control simulations (time stepping) for control verification, the nonlinear AMB force maps are modelled as look-up tables (LUTs) in Matlab Simulink. Voltage and current limitations, control system delays and control discretization are also present in the model. Figure 5 presents the levitation force and inductance of radial AMB computed at various operating conditions in FEM.

C. Drive train model

The MMW, RENK coupling, and Rotatek load machine rotors are modeled as separate FEM models. Each rotor model undergoes the modal reduction where few dominant bending modes are retained. The load model uses the ball bearings and therefore the rigid modes of Rotatek are not included as only its bending can be affected by the forces. The drive train (multi-rotor) dynamic equations are assembled such that ending node locations of all three parts overlap. The resulting state variable form is according to eq. (6). However, the models connect via directional stiffness and damping at the nodes where RENK coupling middle tube connects to the coupling flanges fitted on MMW and Rotatek rotors. The forces transferred between the rotors through the linear stiffness and damping coefficients can be monitored as additional model outputs.

This modular modelling approach is convenient because the control plant can use the same MMW model which is used in the drive train. However, the resulting drive train dynamics are prone to model reduction errors and number of retained dominant modes in each rotor.

An alternative approach would be to model the whole drive train as one structure and then conduct the modal reduction to obtain the control plant model. In such case the free-free mode shapes of the connected drive train are readily accessible but the control MMW plant cannot be obtained directly from the drivetrain model; and model reduction for control purposes is an open question.

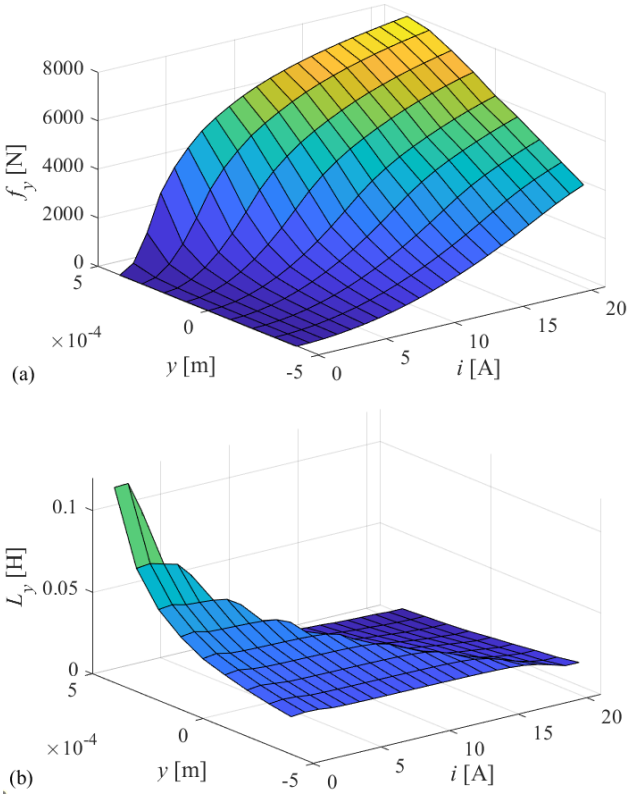

Fig. 5. LUTs of radial AMBs: (a) force map, (b) inductance map, used for time stepping control verification in Matlab prior experiments [14].

III. Control

With the plant model available, different model-based control strategies are possible. The H-inf control or LQG control at fixed speed are the first choices. When accounting for variable speed, the linear parameter-varying (LPV) control or modal control schemes can be used as well. For filtering out synchronous disturbance effects, on measured positions and currents, various unbalance force rejection or synchronized displacement suppression methods can be used as a feed forward or as an added disturbance observer. Here, we show that basic model-based control without any added or advance control features is sufficient if the control plant model is formulated and tuned correctly.

The control plant used in the control synthesis retains the rigid modes of the MMW rotor and its first (dominant) lowest frequency bending mode. In simulations the verification plant uses three bending modes. In general, for non-adaptive LQG and H-inf controllers the control plant with speed closer to zero then to maximum is used for optimal performance in respect to external disturbances.

For the model-based control when 3 radial AMBs are applied the LQG controller with the integral (per axis) cannot tolerate eccentricity in the location of middle radial AMB. Therefore, H-inf controller without integral has to be used. The general control block diagram is presented in Fig. 6.

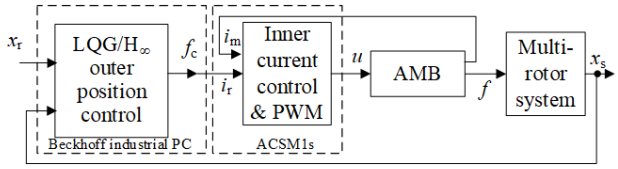

Fig. 6. General applied cascade control architecture. The outer position controller is implemented in the Beckhoff PLC while the inner current controllers are implemented in the FPGAs interfacing to the ABB's ACSM1s.

A. Control simulations

The exemplary cascade control with the model-based LQG position control (synthesised at fixed speed) in the outer loop and the PID control in the inner loops are tested with the accurate nonlinear drive train model. The validation plant has variable speed and it retains several modes in each rotor. The force and inductance LUT nonlinearities, signal saturation, delays, noise etc., are present. The MMW model and the LQG control are adopted from [13] and [1] but the control plant model is updated according to measured drive train dynamics. The validation plant retains the coupled drive train model. After analytical analysis of the closed loop performance and verification in the non-linear simulations the experimental tests are performed.

IV. Experimental results

A. Control plant tuning

The stand alone MMW rotor is commissioned first. With the initial controller the frequency responses of the plant are captured (Fig. 8a). The MMW rotor model is tuned according to the identification results. Then, the additional point mass of the coupling flange (and sleave) is added to the rotor end; and the plant model and controller are recomputed. It is not possible to make identification of stand alone MMW rotor with added point masses as flange is not separable from the coupling tube. The rotors of the drive train are aligned and MMW rotor is levitated while connected via coupling. At this point the frequency responses can be captured for the connected drive train as seen in Fig. 8b.

We have retained as a plant model only MMW rotor (with coupling flange added point mass). This mechanical plant model is tuned such that its bode magnitude frequency responses correspond to experimental measured ones but of the whole drive train. This simplification is possible because of relatively low stiffness coupling.

When tuning the plant model the x and y planes are assumed identical. However, the experimental data gives different responses. The reason for this is in the gravity vector oriented in negative y axis direction. The machine tubing is bolted to the concrete test bench and more rigid along y axes.

B. Experimentation with rotating system

After tuning of the controller when taking into account dynamics of the connected drive train, the rotors are rotated.

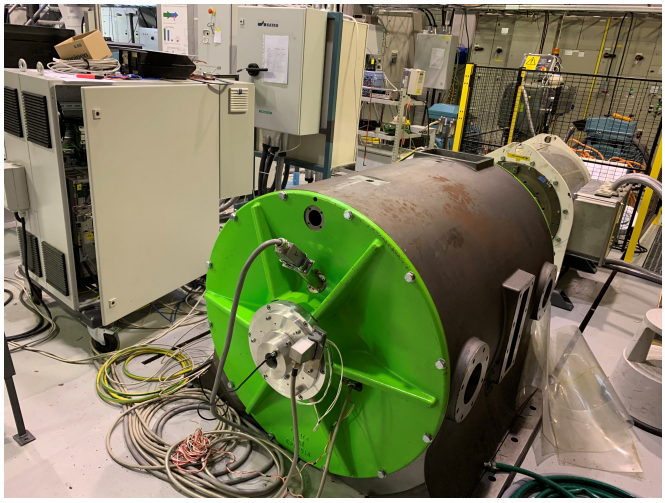

Fig. 7. Drive train with control electronics and inverters cabinets. The MMW has green end tubing plates in front and Rotatek load in back.

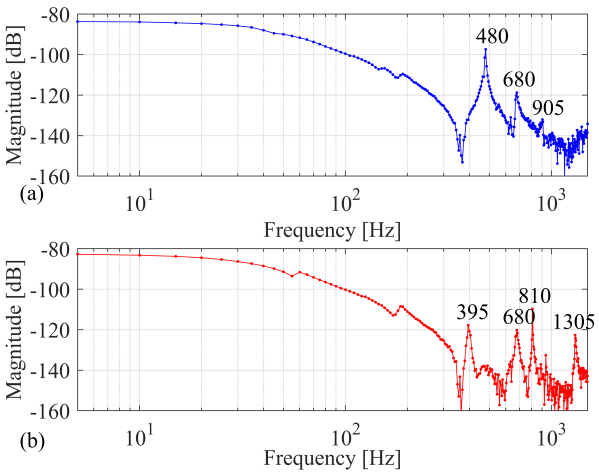

Fig. 8. Measured frequency response magnitudes of (a) MMW rotor without coupling flange and (b) Assembled drive train. The gain from the excitation to the rotor displacement is measured in the planes C and in the x axis.

Figure 9 presents measured orbits and positions of all AMB sensors at 4000 r/min. Figure 10 shows maximum rotor center deviation during rotors acceleration.

V. Discussion

The very compact HS machine, where the application is directly integrated to the electric machine rotor provides best performing machines, however, the design phase is laborious as it requires multiple iterations between different engineer disciplines and the solution scalability is low. In order to provide more scalable solution, which can be used for various loads, the proposed connection coupling is proposed, which can be designed for wider application utilization purposes.

In the modelling of the drivetrain two different modelling methods are considered: modelling of all connected rotors separately and connecting modal reduced models together,

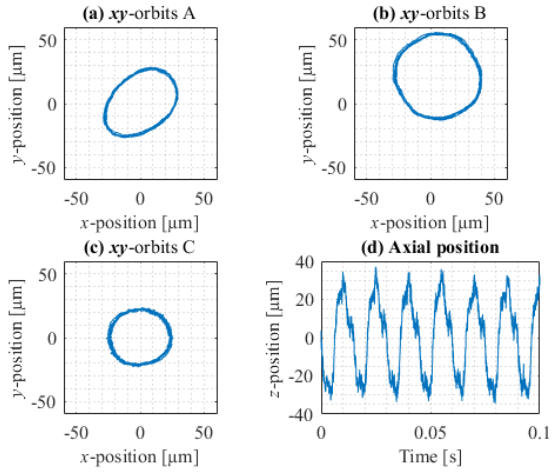

Fig. 9. Measured orbits at 4000 r/min when AMB-rotor connected to external load: (a) sensor A, (b) Sensor B, (c) sensor C, and (d) axial position.

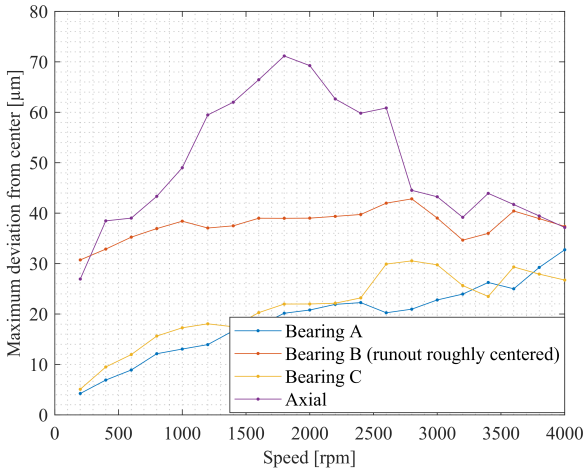

Fig. 10. Measured maximum rotor center deviation from the mean position of rotor in ABC radial sensor planes and in the axial direction during run up speed rump.

and modelling the drive train as a whole. Both described approaches result in the same trend. The eigenfrequencies of the connected structure state matrix are lower compered to the eigenfrequencies of the MMW (AMB-controlled) rotor alone. This is confirmed with the experimental frequency responses.

At higher rotational speeds an influence of a sensor runout (synchronous error in positions during rotation) on the closed-loop AMB-control system can be minimized by employing synchronous compensation (unbalance force rejection). This will reduce orbits, save energy expenditure in AMB currents and alleviate effects of unbalance. Still, with experimental tests up to 7000 r/min there was no need for synchronous compensation in the tested setup with only basic linear model-based AMB controller. Peak of closed loop sensitivity function remained lower than 9 db, which corresponded to requirements for levitating systems according to ISO 14839-3 [22]. The speeds above 7000 r/min have not been allowed because of safety considerations of test facilities.

VI. Conclusions

Analysis, modelling and experimental model and control validation of AMB supported multi-rotor drive train have been shown for the first time.

To handle the changes in the dynamics, the control models have been re-tuned according to frequency responses of the multi-rotor system. The control plant comprising of single rigid rotor but with retained the first bending mode with changed frequency has been applied. It still get good performance indices in terms of measured output sensitivity according to the ISO14839-1 norm.

For the control model the MMW rotor, coupling and application can be modelled separately. After the model reductions as would be done for single rotor, the joint by coupling forces rotor components can be assembled into verification model and used in simulations. However, with reduced number of retained modes the accuracy is compromised.

For most precision the full drivetrain should be modelled. However its utilization directly in the control design is challenging. For the future studies the investigations for the multi-rotor modelling and control design including more then two AMB planes will be in focus.

References

[1] R. P. Jastrzebski, D. Kepsu, A. Putkonen, I. Martikainen, A. Zhuravlev, and S. Madanzadeh, "Competitive technology analysis of a double stage kinetic compressor for 0.5 mw heat pumps for industrial and residential heating," in *2021 IEEE International Electric Machines Drives Conference (IEMDC)*, 2021, pp. 1–7.

[2] Y. Lei, B. Yang, X. Jiang, F. Jia, N. Li, and A. K. Nandi, "Applications of machine learning to machine fault diagnosis: A review and roadmap," *Mechanical Systems and Signal Processing*, vol. 138, p. 106587, 2020.

[3] A. Noshadi, J. Shi, W. S. Lee, P. Shi, and A. Kalam, "System Identification and Robust Control of Multi-Input Multi-Output Active Magnetic Bearing Systems," *IEEE Transactions on Control Systems Technology*, vol. 24, no. 4, pp. 1227–1239, 2016.

[4] D. Bobylev, T. Choudhury, J. O. Miettinen, R. Viitala, E. Kurvinen, and J. Sopanen, "Simulation-based transfer learning for support stiffness identification," *IEEE Access*, vol. 9, pp. 120 652–120 664, 2021.

[5] H. Gao, X. Meng, and K. Qian, "The Impact Analysis of Beating Vibration for Active Magnetic Bearing," *IEEE Access*, vol. 7, pp. 134 104–134 112, 2019.

[6] "Vibration suppression control for AMB-supported motor driveline system using synchronous rotating frame transformation," *IEEE Transactions on Industrial Electronics*, vol. 62, no. 9, pp. 5700–5708, 2015.

[7] S. Zheng, H. Li, C. Peng, and Y. Wang, "Experimental Investigations of Resonance Vibration Control for Noncollocated AMB Flexible Rotor Systems," *IEEE Transactions on Industrial Electronics*, vol. 64, no. 3, pp. 2226–2235, 2017.

[8] "In situ runout identification in active magnetic bearing system by extended influence coefficient method," *IEEE/ASME Transactions on Mechatronics*, vol. 2, no. 1, pp. 51–57, 1997.

[9] A. D. Graham and M. Wimshurst, "The high speed oil free intelligent motor-compressor," in *1993 Fifth European Conference on Power Electronics and Applications*. IET, 1993, pp. 384–389.

[10] N. Uzhegov, E. Kurvinen, J. Nerg, J. Pyrhönen, J. T. Sopanen, and S. Shirinskii, "Multidisciplinary design process of a 6-slot 2-pole high-speed permanent-magnet synchronous machine," *IEEE Transactions on Industrial Electronics*, vol. 63, no. 2, pp. 784–795, 2015.

[11] E. Kurvinen, C. Di, I. Petrov, J. Nerg, O. Liukkonen, R. P. Jastrzebski, D. Kepsu, P. Jaatinen, L. Aarniovuori, E. Sikanen *et al.*, "Design and manufacturing of a modular low-voltage multimegawatt high-speed solid-rotor induction motor," *IEEE Transactions on Industry Applications*, vol. 57, no. 6, pp. 6903–6912, 2021.
[12] D. Kepsu, E. Kurvinen, J. Tiainen, J. Honkatukia, T. Turunen-Saaresti, and R. P. Jastrzebski, "Interdisciplinary design of a high-speed drive-train for a kinetic compressor in a high-temperature heat pump," *IEEE Access*, vol. 9, pp. 143 877–143 900, 2021.
[13] R. P. Jastrzebski, E. Kurvinen, and O. Pyrhönen, "Design, modelling and control of MIMO AMB system with 3 radial bearing planes for megawatt-range high-speed rotor," in *IEEE International Electric Machines Drives Conference (IEMDC)*, San Diego, CA, USA, 2019, pp. 805–811.
[14] R. P. Jastrzebski, A. Putkonen, E. Kurvinen, and O. Pyrhonen, "Design and modeling of 2 MW AMB rotor with three radial bearing-sensor planes," *IEEE Trans. on Industry Applications*, vol. 57, no. 6, pp. 6892–6902, 2021.
[15] P. Kumar and R. Tiwari, "Finite element modelling, analysis and identification using novel trial misalignment approach in an unbalanced and misaligned flexible rotor system levitated by active magnetic bearings," *Mechanical Systems and Signal Processing*, vol. 152, p. 107454, 2021.
[16] P. Kumar and R. Tiwari, "Dynamic analysis and identification of unbalance and misalignment in a rigid rotor with two offset discs levitated by active magnetic bearings: a novel trial misalignment approach," *Propulsion and Power Research*, vol. 10, no. 1, pp. 58–82, 2021.
[17] R. S. Srinivas, R. Tiwari, and C. Kannababu, "Model based analysis and identification of multiple fault parameters in coupled rotor systems with offset discs in the presence of angular misalignment and integrated with an active magnetic bearing," *Journal of Sound and Vibration*, vol. 450, pp. 109–140, 2019.
[18] Z. Sun, Y. He, J. Zhao, Z. Shi, L. Zhao, and S. Yu, "Identification of active magnetic bearing system with a flexible rotor," *Mechanical Systems And Signal Processing*, vol. 49, no. 1-2, pp. 302–316, 2014.
[19] A. Noshadi and A. Zolfagharian, "Unbalance and harmonic disturbance attenuation of a flexible shaft with active magnetic bearings," *Mechanical Systems and Signal Processing*, vol. 129, pp. 614–628, 2019.
[20] H. J. Ahn, S. W. Lee, S. H. Lee, and D. C. Han, "Frequency domain control-relevant identification of MIMO AMB rigid rotor," *Automatica*, vol. 39, no. 2, pp. 299–307, 2003.
[21] H. Nelson, "A finite rotating shaft element using timoshenko beam theory," *Journal of mechanical design*, vol. 102, no. 4, pp. 793–803, 1980.
[22] ISO14839-1:2018, "Vibration of rotating machinery equipped with active magnetic bearings – part 3: Evaluation of stability margin, international standards organization," *International Standard Organisation*, 2006.

BIOGRAPHIES

Rafal Piotr Jastrzebski (Member, IEEE) was born in Lodz, Poland in 1978. He received the M.Sc. degree in electrical engineering from the Technical University of Lodz, Poland, in 2002, and the D.Sc. degree in electrical engineering from the Lappeenranta University of Technology (LUT), Finland, in 2007. He worked as researcher in Poland, Germany, Japan, and Finland. Currently he is a Docent with LUT. His research interests include design, modeling, and control of electric machines, sensors, and power electronics. He has long experience in digital control, system engineering of energy applications, mechatronic systems, active magnetic bearings, magnetic levitation systems, and bearingless machines. From 2013 to 2018, he was an Academy Research Fellow. From 2009 to 2011, he served as an Academy of Finland Postdoctoral Researcher.

Atte Putkonen received the M. Sc. (Tech.) degree in electrical engineering from Lappeenranta-Lahti University of Technology (LUT), Finland, in 2020. Currently he is a doctoral student at the LUT School of Energy Systems. His research interests are identification and control of bearingless machines and active magnetic bearing systems.

Andrei Zhuravlev is a doctoral student at the LUT School of Energy Systems, Lappeenranta–Lahti University of Technology LUT. He received the Master's degree in a double degree program between LUT and Saint Petersburg Electrotechnical University (LETI). He completed his exchange studies in Zhejiang Ocean University, China. His field of interests is control of active magnetic bearings and bearingless machines.

Tuhin Choudhury was born in Seppa, India, in 1989. He received the B.Sc. (tech) degree in mechanical engineering from Sikkim Manipal University, India, in 2011, and the M.Sc. degree in mechatronic system design from LUT University, Lappeenranta, Finland, in 2018, where he is currently pursuing the Ph.D. degree with the Department of Mechanical Engineering. He was a design engineer on the development of medical devices and diagnostic instruments, from 2011 to 2016. His research interests include designing, modeling, and simulation of rotating machines, and the analysis of rotor behavior to understand the root cause of unwanted vibrations, specifically due to unbalance.

Emil Kurvinen was born in 1988. He received M. Sc. (Tech.) and D. Sc. (Tech.) degrees in mechanical engineering from Lappeenranta University of Technology (LUT) in 2012 and 2016, respectively. In 2014-2015 he visited University of Virginia as a Fulbright visiting scholar researching active magnetic bearings. In 2016 to 2017 he served as a engineer, structural dynamics in FS Dynamics Finland Ltd. In 2017-2021 he was as a postdoctoral researcher at LUT. Currently he is Machine Design professor in University of Oulu. He has a solid background in machine design, especially in the design, simulation, analysing of rotating machines. His research interests are rotating machines, especially high-speed machines, digital twins and integration of industrial engineering and management to technology.

Eerik Sikanen received the M.Sc. degree in mechanical engineering and the D.Sc. (technology) degree from LUT University, Lappeenranta, Finland, in 2014 and 2018, respectively. He is currently working as a Postdoctoral Researcher with the Laboratory of Machine Dynamics, LUT. His research interests are high-speed rotor dynamics analysis and general vibration dynamics of rotating machinery. He is mainly concentrating on three-dimensional solid finite element modeling of high-speed machinery and systems including contact and thermomechanical effects.

Juha Pyrhönen (Senior Member, IEEE) was born in Kuusankoski, Finland, in 1957. He received the D.Sc. degree in electrical engineering from the Lappeenranta University of Technology (LUT), Lappeenranta, Finland, in 1991.,He became a Professor of Electrical Machines and Drives in 1997 with LUT. He is engaged in research and development of electric motors and power-electronic-controlled drives. His research interests include development of special electric drives for distributed power production, traction, and high-speed applications, and permanent magnet materials and applying them in machines. He is currently researching new carbon-based materials for electrical machines.